HIGH TEMPERATURES INFLUENCE ON THE REINFORCED CONCRETE PANELS STRENGTH THROUGH THE LIMIT ANALYSIS THEORY

Luisa R. Machado
Vanessa F. P. Dutra
Samir Maghous
luisamrossini@gmail.com
pasa.dutra@ufrgs.br
samir.maghous@ufrgs.br
Universidade Federal do Rio Grande do Sul – UFRGS
Av. Paulo Gama, 110, 90040-060, Porto Alegre/RS, Brazil

Abstract. The constitutive behavior of reinforced concrete (RC) structures is significantly altered when exposed to high temperatures. The high thermal gradients cause deterioration of the thermo-mechanical properties of the materials together with thermal-induced deformations, which in turn modify the geometry of the structure. The aim of the present work is to evaluate the influence of fire occurrence on the stability of the RC panel structures, through the limit analysis theory. By modelling the panel as a beam, determining the interaction diagrams for each time of fire exposure is the first step. The temperature profiles along the sections of the panels are obtained numerically and the interaction diagrams by integrating the concrete and steel strengths along the section with explicit account for the different parameters controlling the problem, such as the section thickness, reinforcement area and concrete compressive strength. The second step consists in determining the deformed configuration of panel and associated distribution of axial and bending moment efforts, considering the second order effects caused by the eccentricity of the self-weight load induced by the thermal deformations. This is achieved by analyzing the thermo-elastic equilibrium of the panel under the combined action of thermal gradient induced by fire and self-weight loading. The analysis is done by overlapping the interaction diagrams of the sections and the distribution of internal efforts along the structure. Several numerical examples are presented to assess the effect of relevant parameters on the overall fire safety of the structure, emphasizing the effectiveness of the approach for design purposes.

Keywords: reinforced concrete panels, limit analysis theory, high temperatures, thermal analysis, fire loading

1   Introduction

Reinforced concrete structures (RCS) can be considerably affected when exposed to high temperatures, especially in fire conditions. The RCS behavior in fire is a very complex subject. Although many studies have been developed in recent years to better understand the influence of high temperatures on this kind of structure, many issues still need to be addressed. The problems that occur when RCS are exposed to high temperatures are mainly connected with progressive degradation of its constituents (concrete and steel) mechanical properties, damage induced by excessive deformation and spalling.

Most of the studies in the literature deal with the fire problem analytically or numerically due to the difficulty of carrying out experiments in this area. Some authors developed methods using interaction diagrams. Caldas *et al.* [1] presented an algorithm for the construction of interaction diagrams for arbitrary sections of reinforced concrete in fire. The diagrams were obtained by a stepwise variation of the deformed configuration of the structures. Moreira *et al.* [2] proposed an analytical method according to the Brazilian standard ABNT NBR 15200:2012 [3], to verify the strength capacities of reinforced concrete rectangular sections when exposed to fire on four sides and subjected to axial forces and biaxial bending moments. Pham *et al.* [4] presented a relatively simple computational procedure to obtain interaction diagrams for concrete walls in fire subjected to axial and bending loads. Based on the limit analysis theory, they demonstrated how the lower and upper bound methods, can be implemented leading to the exact determination of such interaction diagrams. Suaznábar and Silva [5] determined ultimate limit state curves of a short reinforced concrete column under biaxial bending in a fire situation, using the isotherm method of 500 °C, and the temperature profile is obtained analytically, whose method was developed by Wickstrom [6].

In the experimental framework, Crozier and Sanjayan [7] analyzed eighteen reinforced concrete walls under standard fire conditions, varying height and thickness ratios, covering thickness, loading and mixing proportions of the concrete, to investigate the strength capacity of structures, as well as the effect of spalling. Buchanan and Munukutla [8] described a numerical method for calculating the strength of reinforced concrete walls exposed to fire, considering different support conditions.

The purpose of the present study is to investigate high temperatures influence on panels strength through the limit analysis theory (LAT), propose by Salençon [9], which allows the structural design in the ultimate limit state in a straightforward way since it does not consider the loading path and the loading history before the collapse. In this case, the structure failure load/domain is obtained considering compatibility between the equilibrium of the considered system subjected to prescribed loads and the strength of its constituent material. In this work, the overall fire safety of the structure shall rely upon three steps. Modeled as beam element, the local strength capacities of the panel as the loads of panels in fire are described by means of interaction diagrams, which are evaluated in the first step by resorting to the static approach of LAT. It should be noted that evaluation of the overall strength capacities of reinforced concrete in fire requires accounting for the continuous reduction in strength of the constituents (concrete and steel) with temperature increase induced by fire process. In the second step, the deformed configuration of the panel as well as the distribution of axial and bending moment efforts are determined from equilibrium analysis of the structure under combined action of thermal gradient and self-weight loading. Yield design analysis of the panel in its deformed configuration is handled in the last step of the by comparing the distribution of internal efforts determined in the second step to its reduced strength capacities defined by interaction diagrams evaluated in the first step.

2   Statement of the problem and framework of analysis

Panels are characterized for having a thickness much smaller than their height, i. e., they are slender structures. Considering the self-weight as the only load acting on the structure, at ambient temperature (without temperature variation $\Delta\theta = 0$) this load only generates axial compression internal forces N along the height of the panel (Figure 1a). Now assuming that one of its faces is exposed to high temperatures $\Delta\theta > 0$), such as in fire situations (Figure 1b), wide temperature difference occurs between the two element faces, which causes geometry modification due to thermal deformations. The greater

the element slenderness, the greater the effects related to the thermal deformations. As can be seen in Figure 1b, the structure deformation outside its plane $u(x)$ leads to load eccentricity which generate, in addition to the axial compressive forces N, bending moment M.
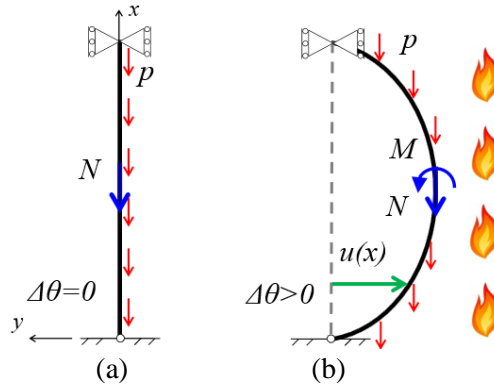
Figure 1. Reinforced concrete panel (a) initial condition and (b) in fire.

Considering structural elements where the normal force N and the bending moment M are the solicitations that govern its rupture, the interaction diagram represents all the concurrent pairs of requesting loads (N, M) supported by its section. Among the direct potential applications of such interaction diagrams is the stability analysis of high rise reinforced concrete panels subjected to fire. Indeed, these conditions will clearly affect the stability of such slender structures in two different ways: the degradation of the panel strength capacities expressed through the reduced interaction diagram on the one hand, the thermal-induced out-of-plane displacements of the panel, which will generate bending moments in addition to compressive loads on the other hand.

It is proposed, for the present work, the verification of these actions together, in order to analyze the stability and failure of reinforced concrete panels, through a simplified one-dimensional approach with a beam-type model (model invariance in relation to the coordinate in the lateral direction), implying, in particular, that the heat flow in the lateral direction is disregarded. It is important to emphasize that a two-dimensional slab model would be a more accurate analysis regarding the evaluation of the boundary effects induced by the lateral panel supports. The adopted model considers the panel connected by a hinged support at its base ($x = 0$) and by a roller at its top ($x = 1$) (Figure 1).

According to Salençon [9], the traditional LAT, the so-called domain K of potentially safe loads (N, M), is the set of loads which can be equilibrated by a stress distribution in the panel (stress tensor fields in the concrete, axial force distributions along the reinforcements), verifying the respective strength conditions at any point of the panel. Therefore, K is defined by the compatibility between the equilibrium and the strength of the constituent material (Eq. 1):

$$N, M \ \in K \Leftrightarrow \begin{cases} \exists \ \underline{\underline{\sigma}} & \text{statically admissible} \\ \underline{\underline{\sigma}} \ \underline{x} \ \in G \ \underline{x} & \forall \underline{x} \in \Omega \end{cases}, \tag{1}$$

where $\underline{\underline{\sigma}}$ the stress field in the solid Ω and $G(\underline{x})$ the convex strength domain of panel constituents. The stress field is statically admissible when satisfies equilibrium ($div \underline{\underline{\sigma}} = 0 \ \forall \underline{x} \in \Omega$), the continuity condition along discontinuity surfaces, the boundary conditions and equilibrates the resulting loads (N, M). The boundary ∂K of this domain, locus of the so-called extreme or failure loads, is called the interaction diagram of the reinforced concrete plate subjected to combined axial and bending loads.

3   Determination of temperature-dependent diagrams

Referring to an orthonormal trihedron frame $Oxyz$, the panel element (Figure 3) is modeled as a parallelepiped solid of thickness b (along the Oy-axis), width a (along Oz-axis) and length l (along Ox-axis). It consists of a supposed homogeneous concrete material, reinforced by n longitudinal steel bars placed along the Ox-direction ($t = \underline{e}_x$). The position of reinforcement layer k of cross-sectional area A_k,

is defined by its coordinate c_k along the Oy-axis, with $-b/2 \leq c_k \leq b/2$.

The element is subjected to the following mechanical loading conditions: (a) body forces (self-weight) are neglected; (b) left hand section ($x = 0$) with stress vector $T \| \underline{e}_x$ related to the resultant axial force $-N\underline{e}_x$ along Ox and bending moment $-M\underline{e}_z$ about Oz; (c) right hand section ($x = l$) with stress vector $T \| \underline{e}_x$ corresponding to the resultant axial force $N\underline{e}_x$ along Ox and bending moment $M\underline{e}_z$ about Oz; (d) remaining horizontal ($y = \pm b/2$) and vertical ($z = \pm a/2$) sides are stress free ($\underline{T} = 0$). The described loading conditions correspond to a panel element with its left hand section in smooth contact with a fixed vertical plate, and its right hand section in smooth contact with a rigid plate in horizontal translation ($\| \underline{e}_x$) associated to a rotation about the Oz-axis. Based upon the above boundary conditions, the loading mode of the element can be determined considering the expressions:

$$N = \int_{x=l} T_x \, dy \qquad M = \int_{x=l} -y T_x \, dy \; . \qquad (2)$$

(a) (b)
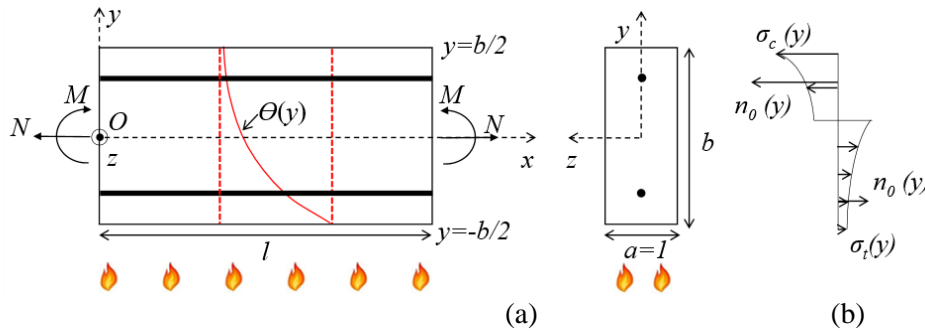
Figure 2. Reinforced concrete panel geometry (a) and limit stress profile function of temperature (b)

Considering the thickness in the Oz-direction unitary, the loading parameters (N, M) can be interpreted as the normal force and the bending moment per unit length along Oz-direction. The strength capabilities of the concrete is characterized by its uniaxial compressive strength $\sigma_c(\theta) < 0$ and its uniaxial tensile strength $\sigma_t(\theta) \geq 0$, being $k_{c,\theta}(\theta)$ and $k_{t,\theta}(\theta)$ decreasing functions of the temperature θ increase and σ_c and σ_t the parameters at ambient temperature:

$$\sigma_c \left(\theta \right) = k_{c,\theta} \left(\theta \right) \sigma_c \qquad \sigma_t \left(\theta \right) = k_{t,\theta} \left(\theta \right) \sigma_t \; . \qquad (3)$$

The reinforcing bars are modeled as linear (i.e. 1D) structural elements embedded in the concrete material described as a 3D continuum. Neglecting their shear and bending resistance, their strength properties will be characterized by the following condition expressed on the axial force n solely:

$$|n| \leq n_0 = \sigma_y \overline{A_k} \; , \qquad (4)$$

where n_0 represents the tensile-compressive strength of the reinforcing bar per unit of the length along Oz, σ_y is the steel uniaxial yield strength and $\overline{A_k}$ the reinforcement rate per unit of the length along Oz. Likewise, the influence of high temperature on steel yield strength is captured through:

$$\sigma_y \left(\theta \right) = k_{s,\theta} \left(\theta \right) \sigma_y \qquad \text{leading to} \quad n_0 \left(\theta \right) = k_{s,\theta} \left(\theta \right) n_0 \; , \qquad (5)$$

where $k_{s,\theta}(\theta)$ is a strength reducing parameter. Although the introduction of a specific strength condition for the reinforcement-concrete interface would not present major difficulties, perfect bonding between the reinforcing bars and the surrounding concrete will be provisionally assumed.

To determine the strength on each point of the section, it is necessary to know the respective temperature. Considering a thermal problem in the fire situation, the heat propagates along the element and, as detailed in Eq. (3) and Eq. (5), the strength properties of the reinforced concrete constituent materials degrade with the temperature increase. As a consequence, the interaction diagram of the panel undergoes changes that depend on the temperature at which the material is subjected.

Therefore, considering the standard temperature versus time curves advocated by design codes (ISO 834:1999) for modeling the action of the fire, a heat transfer analysis may be carried out on the

reinforced concrete panel subjected to a fire applied on its bottom ($y = -b/2$), as sketched in Figure 2a. The temperature field along the panel cross-section is solution to the following thermal boundary value problem defined at time $t > 0$ by:

$$
\begin{cases}
div\ \left(k\,\nabla\theta\ \underline{x} \right)\ + r = \rho\,c\,\dfrac{\partial\theta}{\partial t} & \text{(heat conduction equation)} \\[2mm]
\underline{q}.\underline{n} = 0 \quad \rightarrow \quad \dfrac{\partial\theta}{\partial y} = 0 \quad \text{for } z = \pm a/2 \ , \ t > 0 & \\[2mm]
-k\dfrac{\partial\theta}{\partial y} + h_f\left(\theta - \theta_f\right) = 0 \quad \text{for } y = -b/2 \ , \ t > 0 & \text{(boundary conditions)}\ , \quad (6)\\[2mm]
k\dfrac{\partial\theta}{\partial y} + h_a\left(\theta - \theta_a\right) = 0 \quad \text{for } y = b/2 \ , \ t > 0 & \\[2mm]
\theta(y) = \theta_0(y) \qquad \text{at } t = 0 \qquad \text{(initial condition)} &
\end{cases}
$$

where k is the thermal conductivity, θ is the temperature field, r is the volumetric density of internal heat production, ρ is the mass density, c is the specific heat. In the above equation, $x = (x,y,z)$ refers to the position vector and to time, $\underline{q}$ is the heat flux vector and $\underline{n}$ is the outward unit normal to the boundary surface subjected to heat flow. Quantities h_f and h_a denote respectively the convection coefficients along the face exposed to fire (or temperature θ_f) and along that exposed to ambient temperature θ_a. θ_0 refers to the prevailing temperature before the fire starts.

The first equation in Eq. (6) is the heat equation governing the internal thermal equilibrium equation. The thermal boundary conditions are along the lateral faces $z = \pm a/2$ of the panel are expressing that heat exchange only occurs in the Oy-direction. The thermal boundary conditions along faces $y = \pm b/2$ prescribe the heat flow caused by convection. In the context considered, one-dimensional heat propagation across the plate thickness suggests that the field of temperature increase will depend on the y-coordinate only (Figure 2a). Knowing that the set N and M define the interaction diagram domain K_θ of reinforced concrete panel at different fire exposures, the corresponding values of the loading parameters in equilibrium with the proposed stress distributions may be easily calculated:

$$
N = \int_{-b/2}^{\alpha b/2} \sigma_t\left(y\right)\,dy + \int_{\alpha b/2}^{b/2} \sigma_c\left(y\right)\,dy + \sum_{c < \alpha b/2} n_0(c) - \sum_{c > \alpha b/2} n_0(c)\,, \tag{7}
$$

$$
M = -\int_{-b/2}^{\alpha b/2} \sigma_t\left(y\right)\,y\,dy - \int_{\alpha b/2}^{b/2} \sigma_c\left(y\right)\,y\,dy - \sum_{c < \alpha b/2} c\,n_0(c) + \sum_{c > \alpha b/2} c\,n_0(c)\,. \tag{8}
$$

In order to illustrate the influence of high temperature on interaction diagrams of the reinforced concrete panel, a heat transfer analysis aimed at evaluating the temperature increase across the panel thickness was first conducted considering a rectangular cross section: 0.15 x 1 m². of normal weight concrete with $\sigma_c = 30$ MPa and $\sigma_t = 2.9$ MPa, reinforced with two layers of 10 steel reinforcing 6.3 mm diameter bars with 3 cm of concrete cover at top and bottom and $\sigma_y = 500$ MPa. All analyses are performed considering no internal heat production ($r = 0$). Moreover, the following coefficients were used $h_f = 25$ W/m²°C and $h_a = 4$ W/m²°C in accordance with the NBR 15200 recommendation. In the present study, the thermal problem was numerically modeled by the computational tool Mecway [10] in order to obtain the temperature section profile. Mecway [10] is a finite element analysis package with a focus on mechanical and thermal simulation such as stress analysis, vibration and heat flow. It allows the application of convection and radiation flux boundary conditions, as well as the consideration of thermal and mechanical properties changes according to the temperature at which the material is exposed. The temperature at which the lower face (in fire) is subjected can also vary over time, making possible the use of the standard temperature/time curve specified in ISO 834.

Figure 3a shows the temperature profiles across the thickness obtained by Mecway computer

program calculations, to 0, 60, 90 and 120 min fire durations. The corresponding interaction diagrams, as shown in Figure 3b, could then be determined through the Eq. (7) and Eq. (8).
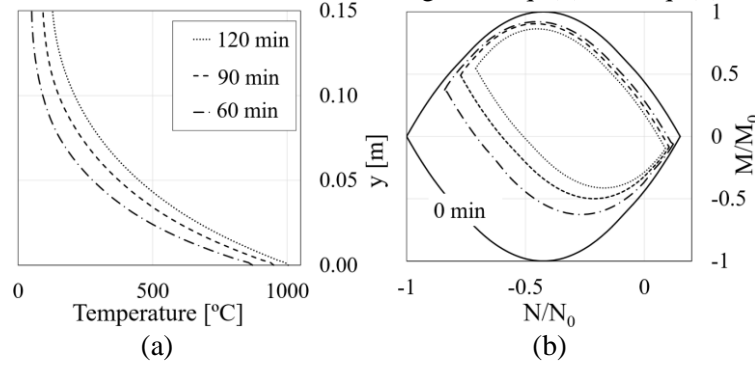
Figure 3. Temperature distributions and interaction diagrams for different fire exposures

As can be seen from this example, the fire exposure leads to an increase of temperature (Figure 3a), resulting in a decrease of material strength parameters and finally to a shrinkage of the interaction diagram (Figure 3b). As one might expect, the longer is the fire duration, the smaller is the size of the interaction diagram and thus the global resistance of the reinforced concrete panel.

4   Panel deformed configuration at thermo-elastic equilibrium

As introduced in section 2, when one of the panel faces is exposed to high temperatures, thermal deformations appear an induce eccentricity of the self-weight load, generating, in addition to N, bending moment M. The estimate of the deformed configuration, that is fundamental for determining the bending moment distribution along the panel in fire, is the focus of this section. As isotropic linear thermoelastic behavior is considered for panel constituent materials, the problem could be divided into two subproblems: thermal (Section 4.1) and mechanical (Section 4.2) problem. The thermal problem does not take into account the element weight, it only considers the thermal deformations associated with temperature elevation. The mechanical problem, however, only takes into account the self-weight and is associated with the elastic deformations caused by its eccentricity.

4.1   Thermal strains and deflection

While panel strains at ambient temperature are purely mechanical, at fire conditions, thermal strains also occur. In addition, thermomechanical deformations/deflections happen due to the restraints of panel supports. The total strain ε is the sum of the thermal strain ε_{th} and mechanical ε_{mec}:

$$\varepsilon = \varepsilon_{th} + \varepsilon_{mec}. \tag{9}$$

Assuming Navier-Bernoulli hypothesis and perfect adherence between concrete and steel bars, the total strain can be estimated by:

$$\varepsilon = \varepsilon_0 - \chi y, \tag{10}$$

where ε_0 is the section geometric center strain and χ is the panel curvature.

Since constituents linear thermoelastic behavior is assumed, the internal efforts on concrete and reinforcement steel bars are, respectively:

$$\sigma - \sigma_0 = E_c \left(\varepsilon - \varepsilon_{th,c} \right), \tag{11}$$

$$n - n_0 = A_s E_s \left(\varepsilon - \varepsilon_{th,s} \right), \tag{12}$$

where σ is the concrete current stress, σ_0 is the concrete initial stress, E_c is the concrete Young modulus

and $\varepsilon_{th,c}$ is the concrete thermal strain. n is the steel stress in the current configuration, n_0 is the steel stress in the initial configuration, A_s is the steel area, E_s is the steel Young modulus and $\varepsilon_{th,s}$ is the steel thermal strain. $\varepsilon_{th,c}$ and $\varepsilon_{th,s}$ are function of the temperature and can be estimated as recommended by ABNT NBR 15200:2012 and ABNT NBR 14323:2013, respectively.

In the purely thermal problem, where only the temperature variation is considered and self- weight is disregarded, the normal stress and the bending moment in the section are null:

$$N - N_0 = \int_A \sigma - \sigma_0 \; dA + \sum_{i=1}^{k} n_i - n_0 \; = 0, \tag{13}$$

$$M - M_0 = -\int_A \sigma - \sigma_0 \; ydA + \sum_{i=1}^{k} n_i - n_0 \; y_i = 0. \tag{14}$$

The section stresses distribution for different fire exposures can be obtained when ε_0 and χ are determined, which can be done through the solution of the Eq. (13) and Eq. (14), considering Eq. (10), Eq. (11), and Eq. (12).

Figure 4a and Figure 4b show, respectively, the section typical total and thermal strains and the typical section stress distribution for 120 min fire duration. The temperature elevation induces homogeneous expansion associated with zero-stress in a solid without constraints. Due to the panel support constraints (Figure 1), the temperature elevation induces tensile stresses in the central region of the cross section while the edge regions become compressed as it can be observed in Figure 4b.

(a)   (b)
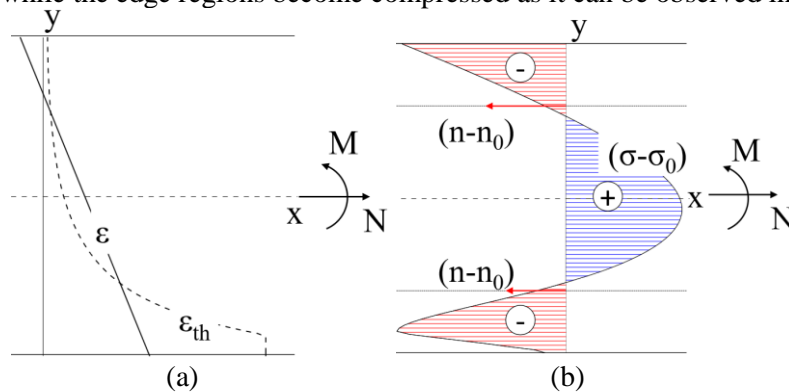
Figure 4. Section total and thermal strains (a) and stress (b) distribution for 120 min fire duration.

As the total strain (Eq. (9)), the total deflection $u(x)$ is the sum of the thermal $u_{th}(x)$ and the mechanical deflection $u_{mec}(x)$. Since the panel curvature, constant for a fire exposure, is related to the deflection second derivative, and considering the boundary conditions $u_{th}(0) = 0$ and $u_{th}(l) = 0$, the thermal deflection is:

$$u_{th} \; x \; = \frac{\chi}{2} x \; x - l \; . \tag{15}$$

4.2   Deflection at structure equilibrium

The total deflection of the panel is evaluated taking into account the second order effects. In this analysis, the structure initial configuration is the panel with thermal deflection $u_{th}(x)$, determined in the previous section. Thus, the linear self-weight load p (Figure 5b) is uniformly redistributed along the thermal configuration (Eq. (15)), causing bending moments.
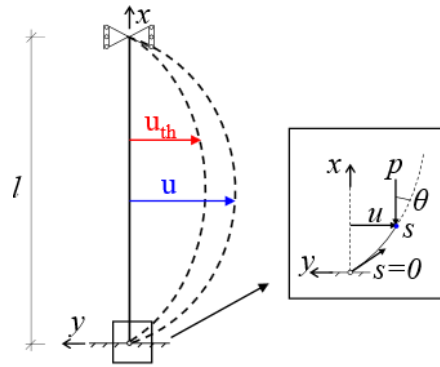
Figure 5. Total u and thermal u_{th} deflection.

In the present study, the axial strain, i.e. the displacements along Ox axis, are neglected. Thus $u(s) = u(x)$, where s and x are the abscissas of the section in the deformed and non-deformed configurations (Figure 5), respectively, and the slope of deformed configuration is defined by $\mathrm{tg}\theta = du/dx$. It is also assumed that the rotations of the cross sections remain infinitesimal, i.e. $|\theta|=|u'(x)|\ll 1$. Therefore, the axial compressive internal force in any panel section is independent of the deformed configuration:

$$N\ x\ = -p\ l-x\ \cos\theta \simeq -p\ l-x\ . \tag{16}$$

The bending moment is evaluated through a isostatic analysis of the panel considering its thermal deformed configuration. The bending moment and the panel deflection are governed by the following coupled equations:

$$M\ x\ = p\left[\frac{x-l}{l}\int_0^l u\ s\ ds + \int_x^l\left[u\ s\ -u\ x\ \right]ds\right], \tag{17}$$

$$M\ x\ =\ EI_{th}\left[u''\ x\ -u_{th}''\ x\ \right], \tag{18}$$

which represent, respectively, the panel equilibrium equation considering its deformed configuration and the panel behavior law. The combination of Eq. (17) and Eq. (18) leads to the differential equation governing the total deflection equation $u(x)$:

$$u'''\ x\ -\frac{p}{EI_{th}}\ x-l\ u'\ x\ =\frac{p}{EI_{th}}u_m, \tag{19}$$

where u_m corresponds to the average displacement along the panel total height. The boundary conditions in this case (Figure 5) are:

$$u\ 0\ = u\ l\ = 0 \quad \text{and} \quad u''\ 0\ = u''\ l\ = \chi_{th}. \tag{20}$$

The problem (Eq. (19) and Eq. (20)) resolution was performed in the present study through the analytical method, making use of a Maple formal software.

Figure 6 compares the obtained thermal and total deflections for a 12 m in height panel.
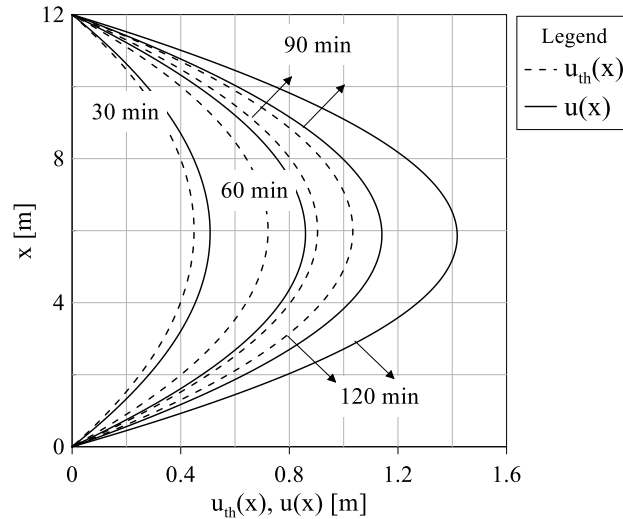
Figure 6. Thermal $u_{th}(x)$ and total $u(x)$ deflections for a 12 m in height panel.

Table 1 shows the thermal strain of the section geometric center $\varepsilon_{0,th}$, the thermal curvature radius $\rho_{th} = 1/\chi_{th}$, the maximum thermal deflection $u_{th,max}$ and maximum total deflection for a panel of 12 m high and different fire exposures. As previously noted in Figure 6, there is a large difference between the panel thermal and the total (second order effects considered) deflections, which increase with temperature rise.

Table 1. $\varepsilon_{0,th}$, ρ_{th}, $u_{th,max}$, and u_{max} for different fire exposures.

Fire exposure [min]	$\varepsilon_{0,th}$	ρ_{th} [m]	$u_{th,max}$ [m]	u_{max} [m]	Difference [%]
30	1.01 x 10⁻³	40.09	-0.45	-0.51	13.3
60	2.00 x 10⁻³	24.95	-0.72	-0.86	19.4
90	2.89 x 10⁻³	19.91	-0.90	-1.14	26.7
120	3.67 x 10⁻³	17.41	-1.04	-1.41	35.6

Finite elements solutions obtained by Pham [11] in the context of a thermo-mechanical analysis at large strains have shown that assumption of infinitesimal adopted in the present analysis proves relevant for the prediction of deformed configuration of the panel.

5 Stability analysis of reinforced concrete panels in fire

In order to evaluate the panel stability, the combination of panel axial-bending loadings should be determined. The axial internal force in any section along the panel height is estimated in the present study by the Eq. (16). The bending moment estimate on the other hand needs the determination of the panel deflection $u(x)$ as can be seen in the Eq. (17). Considering the analytical method, the bending moment distribution can then be rewritten as a function of polynomial series:

$$M\ x\ = p\left[\frac{x-l}{l}\left(-\alpha\sum\frac{a_j}{j+1}\frac{-l/\alpha}{j+2}^{j+2}\right) - \alpha\sum\frac{a_j}{j+1}\frac{\left(\frac{x-l}{\alpha}\right)^{j+2}}{j+2} + \right.$$
$$\left. - l-x\ \sum\frac{a_j}{j+1}\left(\frac{x-l}{\alpha}\right)^{j+1}\right] \qquad (21)$$

$N(x)$ (Eq. (16)) and $M(x)$ (Eq. (21)) are parametric equations whose parameter is the variable x:

$$M\ x\ = \left[\left| \frac{N}{l} \left(-\alpha \sum_{j=0}^{\infty} \frac{a_j}{j+1} \frac{-l/\alpha}{j+2}^{j+2} \right) - \alpha p \sum_{j=0}^{\infty} \frac{a_j}{j+1} \frac{\left(\frac{p}{\alpha N}\right)^{j+2}}{j+2} + N \sum_{j=0}^{\infty} \frac{a_j}{j+1} \left(\frac{p}{\alpha N}\right)^{j+1} \right| \right]. \quad (22)$$

To illustrate, Figure 7 shows the axial-bending loadings for a 12 m in height panel exposed for 120 min to fire. Both the thermal and total deflections are considered. As can be seen, the temperature increase has great influence on the bending moment distribution M_{th}, as well as the second order effects ($M-M_{th}$). Both phenomena must be taken into account in the analysis of the panel stability in fire.
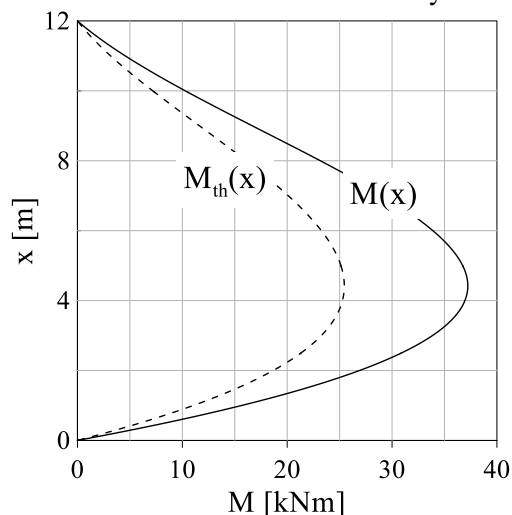
Figure 7. Axial-bending loadings for a 12 m in height panel exposed for 120 min to fire.

To evaluate the panel stability, the interaction diagrams and the axial-bending loadings distributions are superimposed. In this way, as long as the axial-bending loadings (N, M) along the panel is within the interaction diagram or strength domain, the stability of the panel in fire is guaranteed. When the axial-bending loadings distributions becomes tangent or has any points outside the integration diagram, the panel failures. It is important to emphasize, that the panel rupture does not necessarily occur in the section with the maximum bending moment. The point of the load distribution that is tangent to the integration diagram corresponds to the section where the rupture occurs, leading to the general rupture of the structure, since an isostatic beam model is evaluated, and the diagrams are determined by general equilibrium. Therefore, the structure limit load of the corresponds to the rupture load, justifying the adopted thermoelastic analysis.

5.1   Illustrative numerical example

In order to evaluate the influence of high temperature on the stability of reinforced concrete panels, the same section data and constituent materials of the Section 2.2 are considered here, i.e., rectangular cross section: 0.15 x 1 m². of normal weight concrete with $\sigma_c = 30$ MPa and $\sigma_t = 2.9$ MPa, reinforced with two layers of 10 steel reinforcing 6.3 mm diameter bars with 3 cm of concrete cover at top and bottom and $\sigma_y = 500$ MPa. This geometric configuration will be referred as the reference section.

Figure 8a and 8b show the strength domain or interaction diagram K_θ of the reference section and the axial-bending loadings distribution for a panel of 12 m and 6m high, respectively, and 120 min fire duration.

CILAMCE 2019

Proceedings of the XLIbero-LatinAmerican Congress on Computational Methods in Engineering, ABMEC,
Natal/RN, Brazil, November 11-14, 2019
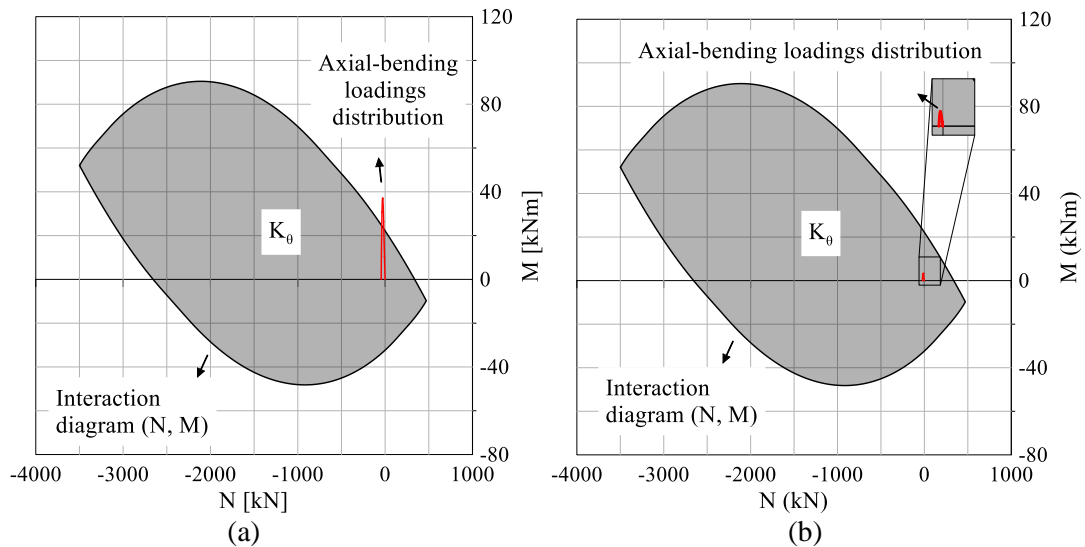
Figure 8. Interaction diagram K_θ of the reference section and the axial-bending loadings distribution for a panel of 12 m (a) and 6m (b) high and 120 min fire duration.

As can be observed in Figure 8a, the axial-bending loadings distribution is not entirely within the section interaction diagram. All points outside K_θ already failed, which indicate that the rupture panel will happen before 120 min fire duration. The 6m panel (same section, same interaction diagram), on the other hand, has all points lying within the section interaction diagram. In this case, all panel sections support the axial-bending loadings caused by the temperature increase and the self-weight eccentricity during 120 min of fire exposure. In the next sections different parameters that act on the reinforced concrete panel stability are evaluated.

5.2   Effect of panel height

First, the influence of the panel height and fire durations on the panel stability are evaluated. Figure 9 shows the interaction diagrams of the reference section and the axial-bending loadings distribution for a panel of different heights and fire durations. As can be seen, for 120 and 90 min, the 12 m panel height fails. For 60 min or less, all analyzed panel heights have the axial-bending loadings distribution entirely within the integration diagram, which indicate the element safety.
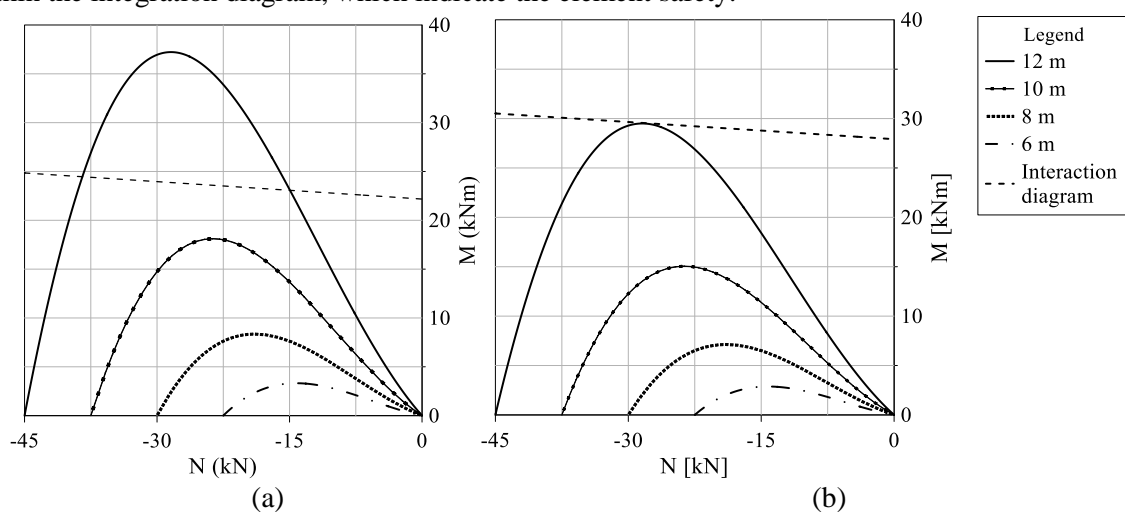
Figure 9. Interaction diagrams of the reference section and the axial-bending loadings distribution for panels of different heights and 120 (a) and 90 (b) min fire duration.

5.3   Effect of concrete compressive strength

The influence of the concrete strength on the interaction diagram and panel axial-bending loadings distribution is evaluated in this section. For this purpose, the reference section and three different concrete compressive strengths, 20, 30 and 40 MPa, are considered in the panel analysis.

Figure 10 shows the "expansion" of reference section interaction diagrams with the increase of the concrete compressive strength. However, panel axial-bending loadings distribution, meanwhile, does not undergo major changes.
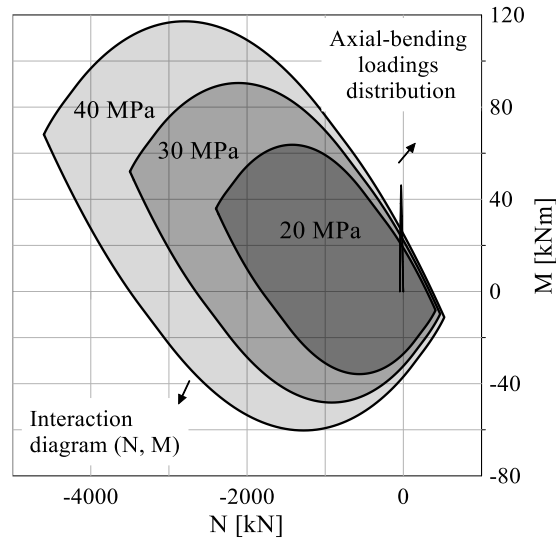
Figure 10. Interaction diagrams and axial-bending loadings distributions for 12 m in height panel and different concrete compressive strengths and 120 min fire duration.

To better illustrate, Figures 11a and 11b show graph zooms of the interaction diagrams and the axial-bending loadings distributions for different panel heights (6, 8, 10, 12m) and different concrete compressive strength (20, 30, 40 MPa), for, respectively, 120 and 90 min fire durations.
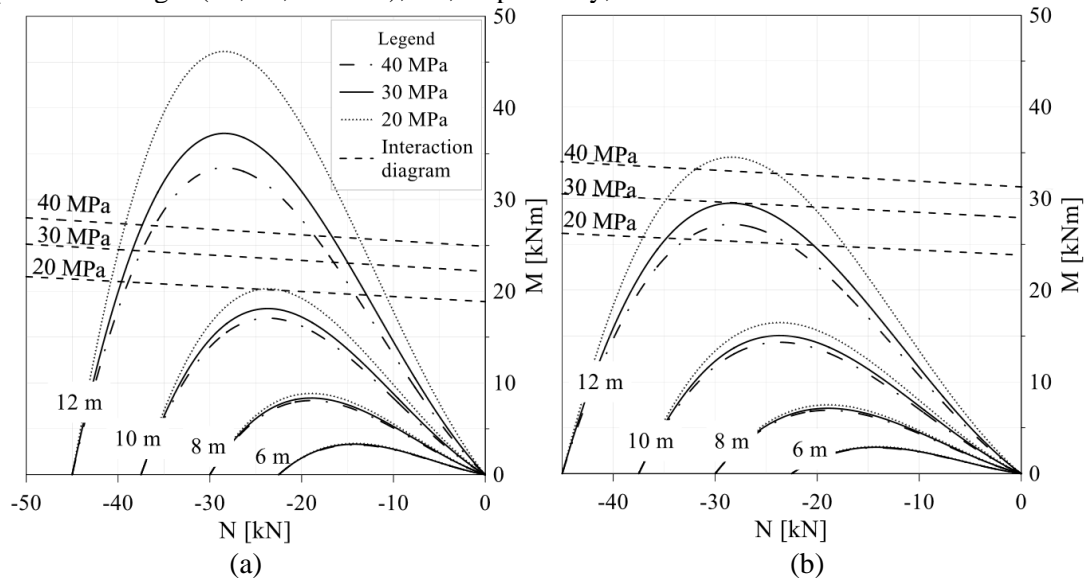
Figure 11. Interaction diagrams and the axial-bending loadings distributions for different panel heights and different concrete compressive strength: (a) 120 and (b) 90 min fire durations.

As can be seen, the greater the panel height, the more significant is the influence of the concrete compressive strength on the axial-bending loadings distributions. Since the concrete Young modulus is a function of the compressive strength, it is expected the axial-bending loadings decrease with the

strength increase, which could be confirmed. Regarding the interaction diagram, at the axial-bending loadings level the compressive strength has slight influence.

5.4   Effect of reinforcement rate

In this section the influence of the reinforcement rate on interaction diagrams and the axial-bending loadings distributions is analyzed. Three different reinforcement rates are considered, A_{s1}, $A_{s2} = 2A_{s1}$ and $A_{s3} = 3A_{s1}$, being A_{s1} the reference section reinforcement area. Figures 12a and 12b show the interaction diagrams and the axial-bending loadings distributions for different panel heights (6, 8, 10, 12m) and different reinforcement rates, for, respectively, 120 and 90 min fire durations.
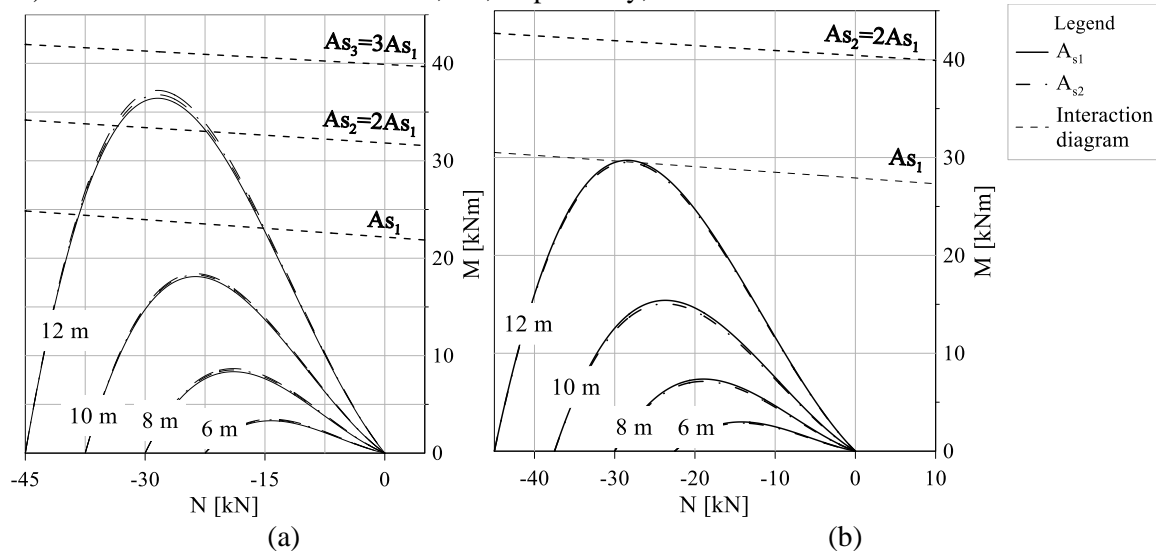
Figure 12. Interaction diagrams and the axial-bending loadings distributions for different panel heights and different reinforcement rates: (a) 120 and (b) 90 min fire durations.

Figure 12 shows that in some cases, the increase of the reinforcement area could avoid the panel failure. This is the case of the 12 m panel height exposed to fire for 120 min, where more than twice the area initially considered is required to the panel stability. In the case of the 12 m panel height exposed to fire for 90 min, twice the area initially considered is enough to the panel stability

The results showed that, in most cases, the reinforcement area does not have a great influence on the axial-bending loadings distributions. The reinforcement bars have no great influence on the temperature distribution along the section, which is basically determined by the concrete area, and thus has insignificant influence on the deflection and the bending moment of the panel. The reinforcement has in fact great influence on the section strength criterion, the increase of the reinforcement area increases the section interaction diagram.

5.5   Effect of panel thickness

In this section the influence of different panel thicknesses on the interaction diagrams and the axial-bending loadings distributions is analyzed. For this purpose, a 12 m panel height exposed to fire for 120 minutes is evaluated. Figure 13 shows the total deflections. Figure 14a and 14b show the influence of panel thickness on the interaction diagram and the axial-bending loadings distributions of panels with six different thickness (15, 16, 17, 18, 19, 20 cm).

The thickness increase leads to strength increase as shown in Figure 14a, the integration diagram (or section strength) expand with the panel thickness increase. Moreover, the results presented in Figure 13 indicate that the thickness has great influence in the panel deformed configuration. This occurs because, when the section thickness increases the panel section bending stiffness also increase, and consequently the deflection and the bending moment decrease (Figure 14b). Finally, when the section thickness increases, the axial internal force also increases (Figure 14b) due to the self-weight increase.
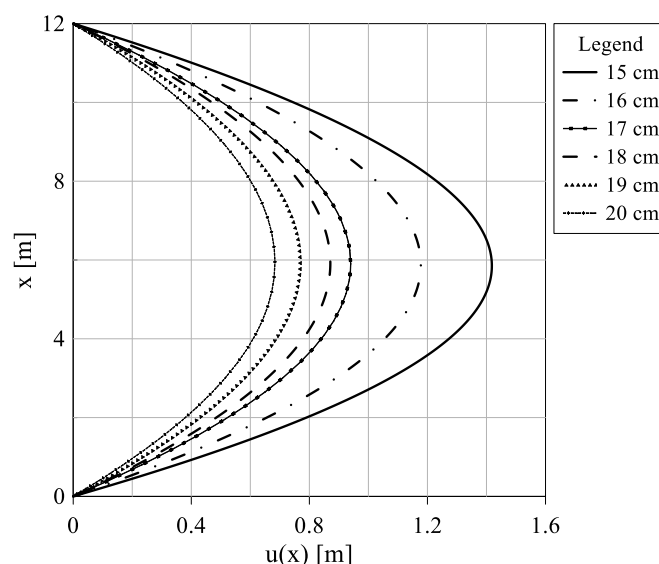
Figure 13. Total deflections of 12 m in height panels with different thickness exposed for 120 min.
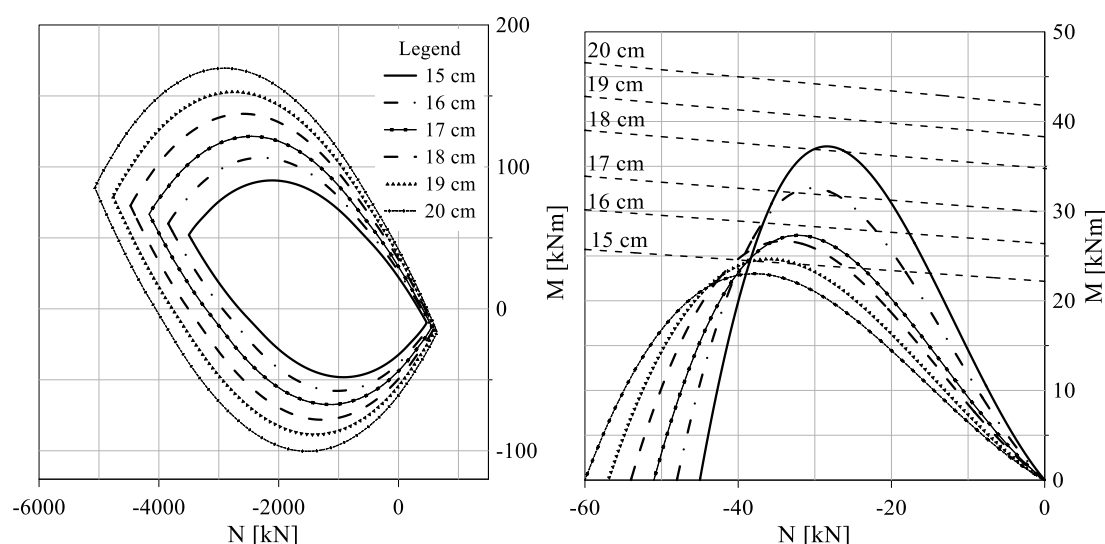
Figure 14. Interaction diagrams of 12 m in height panels (a) and axial-bending loadings distributions (b) with six different thickness exposed to fire for 120 min.

The results in Figure 14b indicate that for 120 min a panel 12 meters with 15 cm or 16 cm thicknesses will fail. In these cases, some axial-bending loadings exceed the strength limit, indicating the structure rupture. The other evaluated thicknesses (17, 18, 19 and 20 cm), the axial-bending loadings distributions are completely within the respective interaction diagrams. As already mentioned, the thickness increase improves the panel strength and also causes significant reduction of the panel bending moments. The results also indicate that small thickness changes could lead to a safety condition, as it can be seen when the thickness changes from 16 to 17 cm (Figure 14b). This section presents results for panel exposed to fire only for 120 min. All the other configurations could be however evaluated and for each case the panel stability verified.

6 Conclusions

This work proposed a method for assessing the stability of reinforced concrete panel in fire based on limit analysis theory. The method relies upon the determination of the interaction diagrams which depend mainly on the fire exposure time as well as on the panel cross-section geometry and on thermo-

mechanical properties of the constituents (concrete, steel bars) that evolve continuously with the temperature increase. The reasoning also requires assessment of deformed configuration of the panel and associated distributions of axial-bending efforts. The latter distributions have been obtained from thermo-elastic equilibrium analysis of the panel. Analytical solution for the panel deformed configuration has been determined analytically taking into account the effects of the self-weight eccentricity induced by the temperature increase. The proposed analysis allows for direct and easy evaluation of the stability conditions of reinforced concrete panels, thus providing an effective method for intensive parametric studies and design of structural fire safety. From a theoretically viewpoint, the analysis based on the limit analysis tools emphasized its aptitude to properly capture the essential features of strength reduction connected with temperature increase and reflected at the overall interaction diagrams. In addition, the numerical applications have shown the relevancy to incorporate in the analysis the second order effects, notably for the determination of bending moment distribution.

The analysis also pointed out how small changes in the panel geometry (height and thickness) can have strong influence on the stability conditions of the panel in fire. It is important to emphasize that although the panel height does not affect the interaction diagrams, it however strongly affects the bending moment distribution. Considering, for instance, 120 min of fire duration, the maximum bending moment of a panel of 12 m is twice and 11 times greater than that of a panel of 10 and 6 m in height, respectively. Regarding the panel thickness, besides having significant influence on the interaction diagram, also meaningfully affects the axial-bending loadings distribution. As the thickness increases, the structure weight increases so the axial force does. On the other hand, the bending moment decrease, because of the stiffness increase that affects the deflection and, consequently, the bending moment.

It is also possible to conclude from the developed study that, although the reinforcement rate increase does not significantly affect the axial-bending loads distribution, it considerably improves the interaction diagram. The benefits of this panel strength enhancement with the reinforcement increase is not so advantageous because the solicitation distributions of the evaluated structures are in a region of the interaction diagram (neutral axis is above the upper reinforcement, and the section is predominantly in tensile stress) where this enhancement is not as pronounced.

Regarding the evaluation of the concrete compressive strength influence, it is possible to observe that once the concrete strength increases, its Young modulus also increase and consequently the deformation and the bending moment distribution decrease. Besides that, the concrete compressive strength increase also allows the strength capacities improvement or the interaction diagram "expansion". In spite of the limitations of this work: (a) analysis simplification through a beam model, (b) validation with experimental results were not performed here and (c) exact determination of the fire duration that leads to panel failure being not possible with proposed methodology, it allows designers to predict in a relatively simple and direct way the safety condition of reinforced concrete panels in fire.

References

[1] R. B. Caldas, J. J. Souza and R. H. Fakury. Interaction diagrams for reinforced concrete sections subjected to fire. *Engineering Structures*, 32, pp. 2832–2838, 2010.
[2] A. M. M. Moreira, N. A. Silva and R. M. Silva, Verificação de seções retangulares de concreto armado submetidas à flexão oblíqua composta em situação de incêndio. *CILAMCE*, 2013.
[3] ABNT NBR 15200. Projeto de estruturas de concreto em situação de incêndio: procedimento. 2012.
[4] D. T. Pham, P. de Buhan, C. Florence, J. V. Heck and H. H. Nguyen. Interaction diagrams of reinforced concrete sections in fire: a yield design approach. *Engineering Structures* 90, pp. 38–47, 2015.
[5] J. S. Suáznabar. and V. P. Silva. Método simplificado para análise termestruturais de pilares curtos de concreto armado em situação de incêndio**.** *Congresso Ibero-Latino-Americano sobre Segurança contra Incêndio*, 2017.
[6] U. Wickstrom. Temperature calculation in fire safety engineering. Springer. 2016.
[7] D. A. Crozier and J. G. Sanjayan. Tests of Load-Bearing Slender Reinforced Concrete Walls in Fire. *ACI Structural Journal,* 97, pp. 243-251, 2000.

[8] A. Buchanan and V. R. Munukutlha. Fire Resistance of Load-Bearing Reinforced Concrete Walls. *Fire Safety Science*, 3, p.p 771– 780, 1991.

[9] J. Salençon. Yield design. ISTE Ltd and John Wiley and Sons, Inc, 2013.

[10] Mecway. Manual- Mecway Finite Element Analysis, Version 9.0, 2018.

[11] D. T. Pham. Analyse par le calcul à la rupture de la stabilité au feu des panneaux em béton armé de grandes dimensions, PhD thesis, Université Paris-Est, 2014.